ASM Sc. J., 12, Special Issue 4, 2019 for ICSE2018, 83-89

Electrical and Structural Characterization of Graphene Carbon Nanotubes Hybrids (GCH) Structures

Lee Li Theng[1], Iskandar Yahya[1,2], Mahamad Fariz Mohamad Taib[3], Mohd Ambri Mohamed[1*]

[1]*Institute of Microengineering & Nanoelectronics, Universiti Kebangsaan Malaysia, 43600 Bangi, Selangor, Malaysia.*

[2]*Faculty of Engineering and Built Environment, Universiti Kebangsaan Malaysia, 43600 Bangi, Selangor, Malaysia.*

[3]*Faculty of Applied Science, Universiti Teknologi Mara, 40450 Shah Alam, Selangor, Malaysia.*

Graphene carbon nanotubes hybrids (GCH) structure helps prevent graphene film from stacking together and provide a more conductive path compared to pristine graphene and pristine carbon nanotubes (CNT). In this paper, simulation on the energy band gap and density of states are carried out using Material Studio software. Then, we fabricated samples which consist of pristine graphene, pristine CNT and graphene carbon nanotubes hybrids (GCH) structure respectively. The presence of graphene and CNT are confirmed by Raman spectroscopy and field-emission scanning electron microscope. Furthermore (FESEM). Electrical characteristics (I-V) were performed on electrodes with GCH on top of it. The results are compared with pristine graphene on the electrode and pristine CNT on the electrode. The result shows that GCH has much higher conductivity as compared to pristine graphene and pristine CNT. Thus, GCH structures have enhanced the conductivity than pristine graphene and carbon nanotubes. This behavior makes it a promising candidate as electrode material.

Keywords: Graphene; Carbon Nanotube; hybrids; graphene carbon nanotubes hybrids; electronics.

I. INTRODUCTION

Carbon nanotubes (CNT) and graphene have attracted great attention among researchers because of their remarkable and supreme properties such as exceptionally high electronic conductivity and mechanical strength. However, due to their nanoscale size, CNTs and graphene face limitation such as the problem of dispersion and stacking that will further reduce their specific surface area and electric conduction ability [1-3].

Carbon nanotubes are a one-dimensional structure while graphene is a two-dimensional structure. Thus, a solution is proposed to make three-dimensional graphene carbon nanotubes hybrids (GCH) structure through the hybridization of carbon nanotubes and graphene. This 3D GCH can provide its function as a bridge from microscopic CNT and graphene to macroscopic devices to allow electron transfer in order to form a better interconnected conducting network transfer [4-6,14]. Moreover, this 3D GCH structure can extend their applications without introducing non-carbon impurities.

Several strategies and techniques have been reported to fabricate GCH up to now. These methods include post-organization technique [7-8] and direct growth using chemical vapor deposition (CVD) [9-10]. Both methods have their advantages. The post-organization method is relatively simpler and requires less cost than the CVD process. However, it still shows promising results in terms of electronics and mechanical properties. CVD process is more complicated but showing a possibility for the formation of covalent C-C bonding.

With respect to the above-mentioned considerations, this project aims to fabricate a three-dimensional graphene-carbon nanotubes hybrids structure using the post-organization process, where GCHs structures were dispersed on a substrate. Comparison of the electrical conduction between pure graphene, pure carbon nanotubes and graphene-carbon nanotubes hybrid structure are carried out. Besides, simulation is also performed among the three materials to make a prediction

*Corresponding author's e-mail: ambri@ukm.edu.my

of the behavior of GCH material in terms of the energy band gap and density of states. Finally, simulation results are compared to experimental results.

II. MATERIALS AND METHOD

A. BIOVIA Material Studio Simulation

CASTEP in BIOVIA Material Studio software is chosen to do the calculation of energy band gaps and the density of states in this project. Calculation on pristine graphene, armchair, zigzag, and chiral CNTs, and different combination of GCH structure with and without covalent bond are performed In Material Studio, Density functional theory (DFT) is used for the calculations. Perdew, Burke and Ernzerhof (PBE) functional which belongs to the class of generalized gradient approximation (GGA) is used in this work. Ultrasoft pseudopotentials are used in the CASTEP calculation. Before the band structure and density of states are calculated, all configurations are first fully relaxed to reach its minimum energy structures. A k-points set of fine quality was used and the maximum SCF cycles are set to 9999 to ensure the structure reaches the minimum energy states before the calculations end. A 1 x 1x 1 Monkhorst-Pack grid of k-points was employed for the Brillouin-zone integrations.

B. Fabrication of Devices & GCH Samples Preparation

A few field-effect transistor devices are prepared using a standard photolithography process. As fabricated devices consist of pairs of source-drain electrodes with a channel gap of 5 μm, 10μm, 1 5μm, and 20 μm. Chrome (Cr) and Gold (Au) are deposited using a sputtering technique for the source and drain electrodes. The thickness of Cr is 10 μm while Au is 80 μm.

Three different samples are prepared which is pristine graphene on the electrode, pristine CNT on the electrode, and GCH on the electrode. Single- and double-layer CVD graphene on copper (Cu) foil is purchased from Graphene Supermarket. Purchased graphene is transferred on top of the fabricated electrode using the PMMA method for the first sample. Then, another sample is prepared by dip-coating in arc-discharge CNT in deionized (DI) water at 10 mm/min for 5 times. The third sample has graphene transferred on it first, followed by dip-coating in the same CNT solution [15].

C. Optical & Electrical Characterizations

The as-prepared sample was subjected to Thermo Scientific DXR2xi Raman spectroscopy to ensure the presence of graphene and CNTs. The wavelength of 532 nm and 10 mW laser are used for both graphene and CNTs. High-resolution FESEM Merlin Compact is also performed to visualize the structure of graphene and CNTs. Finally, I-V characteristics were carried out using Keithley 4200-SCS to measure the conductivity of each sample. Details of measurement set-up were published in an earlier report [12].

III. RESULTS AND DISCUSSION

A. Energy Band Gap Simulation

Energy band gap calculation on the different type of CNT with the graphene sheet is performed. We choose 4 semiconducting CNTs and 4 metallic CNT with a diameter range from 6 Å to 12.5 Å. From Figure 1, it is shown that all of the GCH structure with semiconducting CNTs has a lower energy band gap compared to its pristine CNT. The type of CNT is identified by (n,m) where n and m are the integers of the vector equation of how the CNT is rolled up. If n=m, it is an armchair CNT. If m=0, it is a zigzag CNT. If n≠m, it is a chiral CNT. For metallic CNT GCH structures, GCH (12,3) shows a lower band gap compared to pristine CNT while all other GCH with metallic CNT shows a larger band gap compared to pristine CNT. However, the increase in band gap for GCH (9,0) is very small and almost negligible. GCH (6,6) and (9,9) show an obviously larger band gap after combine with a graphene sheet. Both of them are armchair CNTs. To verify this, calculations are performed on another armchair CNT with chirality (7,7). The result shows that the band gap of its GCH had increased too. Thus, it can be observed that the change in band gap is correlated to the chirality of CNT attached to the graphene and the GCH structure with armchair CNT will increase the band gap compared to its pristine CNT.

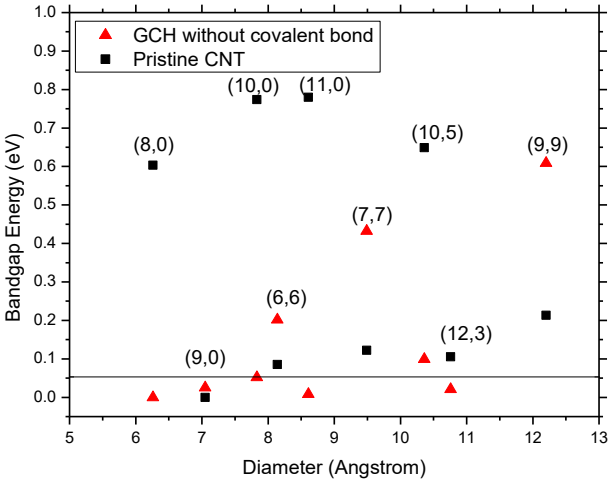

Figure 1. Comparison of energy band gap for GCH without covalent bond with pristine CNT

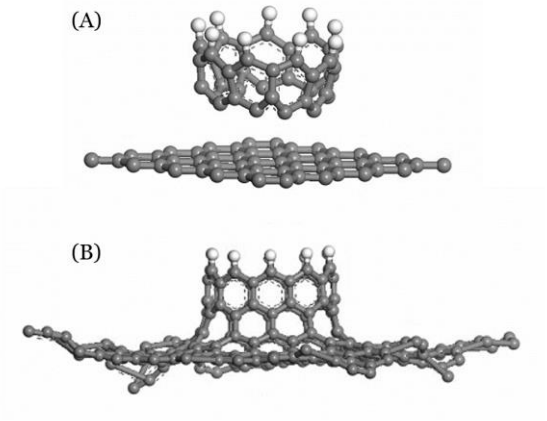

Figure 2. (a) Modelled GCH structure without covalent bond; (b) Modelled GCH structure with a covalent bond

The GCH modeled in Figure 2(a) is without covalent bond in between the interface of CNT and graphene. Next, we also performed the calculation on the GCH structure with a covalent bond at the interface of CNT and graphene as shown in Figure 2(b). However, not all CNT is able to form a stable GCH structure with a covalent bond. Among the GCH structures without covalent that we had performed calculations, CNT (10,5), (12,3) and (9,9) failed to form a stable GCH structure with covalent bond. It fails to reach a minimum energy state which is stable to run for further calculations. It is believed that CNT (10,5) and (12,3) are chiral CNT which have a more complicated arrangement of carbon atoms compared to the armchair and zigzag CNTs while CNT (9,9) has a large diameter than common CNT which is usually less than 10 Å. All the GCH structures with covalent bond have a smaller band gap compared to GCH structure without covalent bond and pristine CNT as shown in Figure 3. Except for GCH (9,0), its GCH structure with covalent bond has a slightly larger band gap compared to GCH without covalent bond. However, the increase in band gap is so small. The presence of covalent bond provides a path for an electron to pass through easily from CNT to graphene. Thus, the GCH structure has a smaller band gap which makes the electron pass through from valence band to conduction band easily.

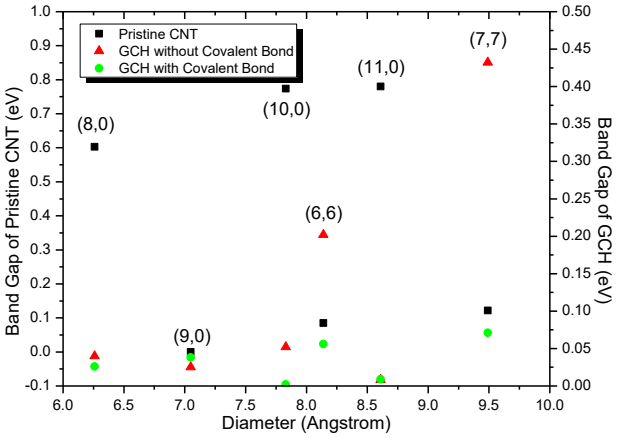

Figure 3. Comparison of energy band gap between GCH with a covalent bond, GCH without covalent bond and pristine CNT

B. Resonance Raman Spectroscopy

Next, Raman spectroscopy is performed on a silicon wafer substrate where CNTs were fabricated by chemical vapor deposition (CVD) method was spin-coated on the surface of the substrate. From the Raman spectra, as shown in Figure 4, we can estimate the diameter of CNTs from radial breathing mode (RBM) [11]. It was around 1.2 to 1.3 nm. Furthermore, we can also estimate the quality of the CNTs by calculating the value of I_D/I_G (I_D = Intensity of D peak; I_G = Intensity of G peak). The defect in this sample is very low at about 0.02 to 0.04.

Figure 5 is the Raman spectra of transferred graphene on Si/SiO_2 substrate. From the spectrum, we can observe that the sample consists of single- and double-layer graphene

indicated by the value of I_G/I_{2D}. If the value is around 0.5, it is single-layer graphene. The higher the value, the more the layer of graphene. Furthermore, it has a very low D peak which indicates that it is very good quality graphene with very low defects even after transferring from Cu foil to substrate. The value of I_G/I_D and I_G/I_{2D} are tabulated in Table 1.

After that, we transferred CNTs to the top of the graphene layer and perform Raman spectroscopy. RBM peaks are observed as shown in Figure 6. The combination of RBM peaks, G-band, and 2D band indicates that CNTs had successfully transferred on top of graphene layers.

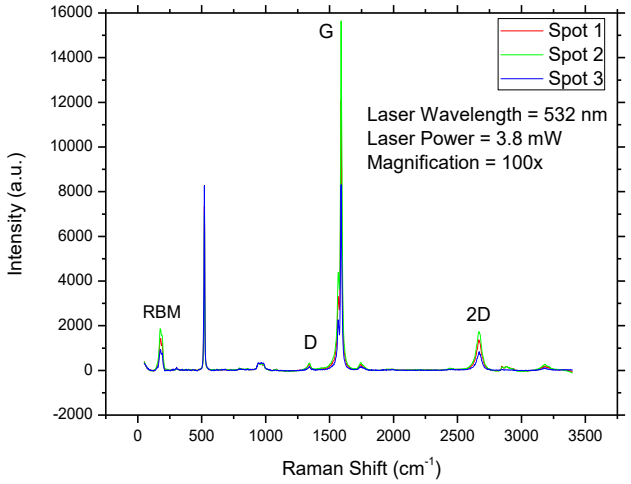

Figure 4. Raman spectrum of transferred CVD CNTs on Si/SiO_2 substrate

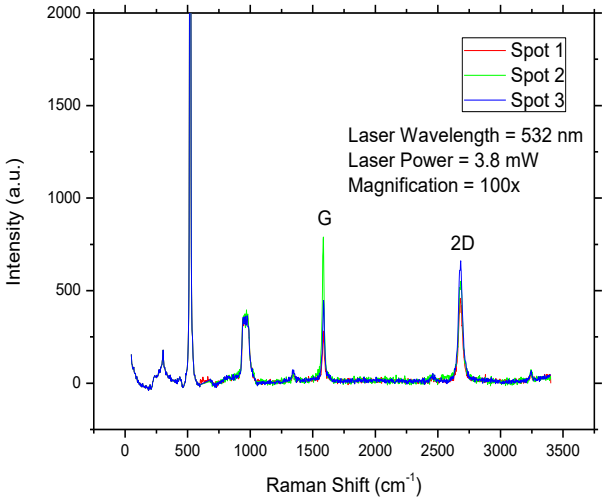

Figure 5. Raman spectrum of transferred graphene on Si/SiO_2 substrate

Table 1. Intensity ratio information from graphene Raman spectra peaks

Spot	I_G/I_D	I_G/I_{2D}
1	0.03	1.43
2	0.28	0.67
3	0.17	0.61

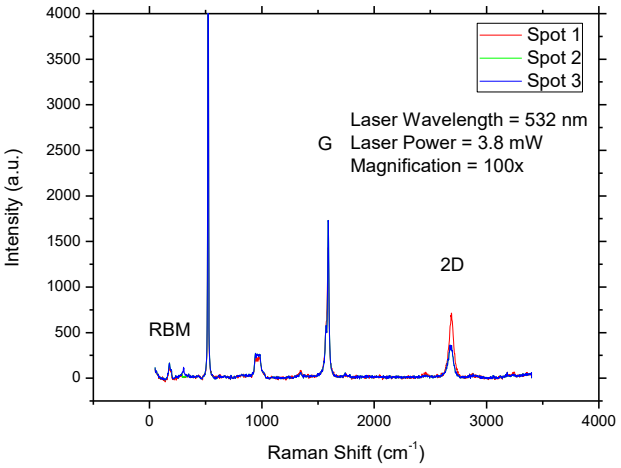

Figure 6. Raman spectrum of GCH structure on Si/SiO_2 substrate

C. Field Emission Scanning Electron Microscope (FESEM) Image

High-resolution FESEM Merlin Compact is used to visualize the dispersion of graphene and CNTs. Figure 7 shows the image of graphene flakes deposited on Si/SiO_2 substrate. We can observe that graphene flakes are folded that might have occurred during the transfer process. This phenomenon explained the detection of double-layer graphene in Raman spectra. CNTs are well dispersed all over the surface of SiO_2 as shown in Figure 8. Lastly, Figure 9 shows the visualization of the GCH structure. The wrinkled structure below CNTs is graphene flakes. CNTs form a well disperse network connection on top of the graphene layer.

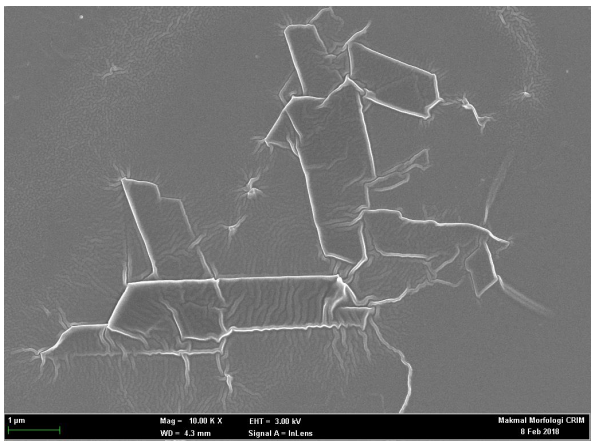

Figure 7. Graphene flakes deposited on Si/SiO_2 substrate

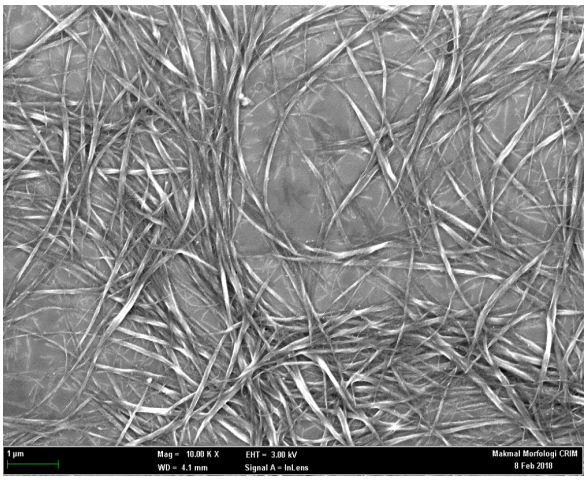

Figure 8. Carbon nanotubes deposited on Si/SiO_2 substrate

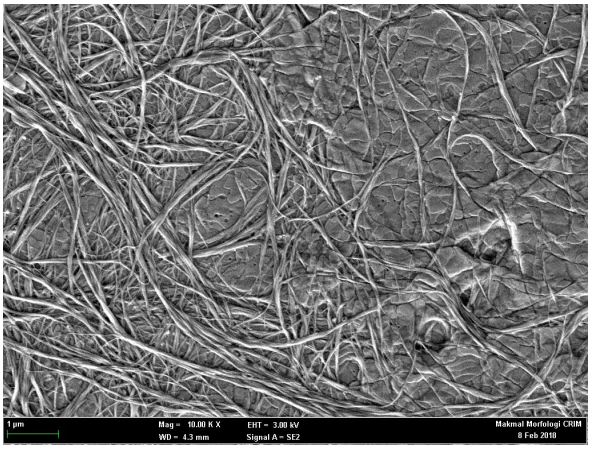

Figure 9. GCH deposited on Si/SiO_2 substrate by post organization process

D. Electrical Characteristics

We fabricated devices consists of 8 pairs of source-drain electrodes with various channel gaps of 5 µm, 10 µm, 15 µm, and 20 µm. I-V characteristics is performed using two probe measurements. As shown in Figure 10, the electrode with GCH shows an increment of conductivity by 4-folds compared to only graphene and an increment of 2-folds compared to that of only CNT. This is due to the increase in the number of conductive paths offered by the GCH hybrids structure. CNT is a one-dimensional material while graphene is a two-dimensional material. With the combination of both, a GCH becomes a three-dimensional material which offers electron to pass through in all directions. There is a reduction in resistivity for GCH compared to graphene and CNT which contribute to its carrier enhancement. The resistance of each material is calculated from the I-V curve and tabulated in Table 2. The resistance value of GCH in this work is 366.3 Ohm which is lower than the reported value by Maarouf et al. which is 380 Ohm [13].

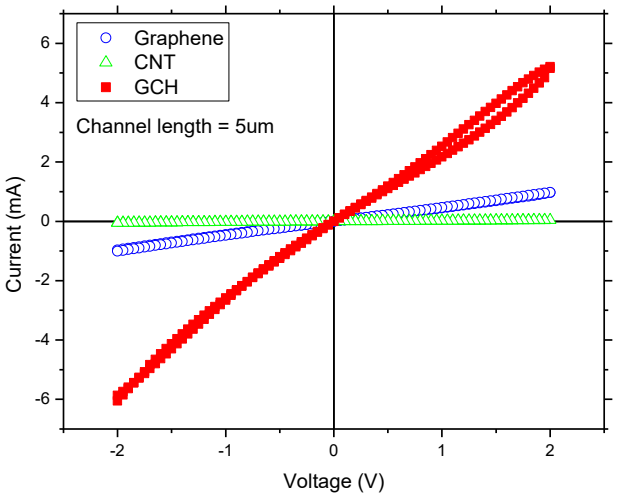

Figure 10. I-V characteristics of graphene, CNT, and GCH

Table 2. Calculated resistance of GCH, pristine graphene and pristine CNT

Material	**Calculated Resistance (Ohm)**
Graphene-Carbon nanotubes Hybrid (GCH) structures	366.3
Pristine Graphene	746.0
Pristine Carbon Nanotubes	18181.8

IV. CONCLUSION

We have predicted the density of states and band gap of GCH structures based on a first-principal calculation using Materials Studios software. It shows that the GCH structure with semiconducting CNTs has a lower energy band gap compared to its pristine CNT. GCH structures give better electrical conductivity by 4-folds as compared to pristine graphene and enhancement of conductivity by 12-folds compared to pristine CNTs. This characteristic makes it an ideal candidate for electrode material. Common electrode materials such as copper is very heavy. This is a disadvantage which makes electronic device becomes heavy and bulky. However, the GCH structure is very light material as it is only made up of carbon. Therefore, GCH material can be a potential candidate as electrode material in nano-scale devices because of its light-weight while offering a high electrical conductivity compared to CNT and Graphene.

V. ACKNOWLEDGEMENT

This work is supported in part by research grants GUP-2018-082 from Universiti Kebangsaan Malaysia and Fundamental Research Grant Scheme FRGS/1/2015/TK04/UKM/02/2 from the Ministry of Education Malaysia.

VI. REFEREENCES

Ani, MH, Kamarudin, MA, Ramlan, AH et al. 2018, A critical review on the contributions of chemical and physical factors toward the nucleation and growth of large-area graphene, *J Mater Sci* vol. 53, no. 10, pp. 7095–7111.

Azam, MA et al. 2017, Review—critical considerations of high quality graphene synthesized by plasma-enhanced chemical vapor deposition for electronic and energy storage devices, *ECS Journal of Solid State Science and Technology*, vol. 6, no. 6, pp. M3035-M3048.

B, Zeng 2016, The synthesis of carbon nanotubes/graphene hybrid with flower-like structure and its application. *Journal of Materials Science: Materials in Electronics*, vol. 27, no. 10, pp. 10421-10426.

Dresselhaus, M, Jorio, A, Souza Filho, A, Dresselhaus, G & Saito, R 2002, Raman spectroscopy on one isolated carbon nanotube, *Physica B: Condensed Matter*, vol. 323, no. 1-4, pp. 15-20.

Kim, Y, Song, W, Lee, S,Jeon, C, Jung, W, Kim, M, & Park, C 2011 Low-temperature synthesis of graphene on nickel foil by microwave plasma chemical vapor deposition. *Applied Physics Letters*, vol. 98, no. 26, pp. 263106.

Liu, J, Zhang, L, Wu, H, Lin, J, Shen, Z & Lou, X 2014, High-performance flexible asymmetric supercapacitors based on a new graphene foam/carbon nanotube hybrid film. *Energy Environ. Sci.*, vol. 7, no. 11, pp. 3709-3719.

Maarouf, AA, Amal, K, Bhupesh, C & Glenn JM 2016, A graphene–carbon nanotube hybrid material for photovoltaic applications, *Carbon*, vol. 102, pp. 74-80.

Mohamed, MA, Azam, MA, Shikoh, E & Fujiwara, A 2010, Fabrication and characterization of CNT-FET using ferromagnetic electrodes with different coercivities, *Jpn. J. Appl. Phys*, vol .49, no. 02BD08.

Ooi, PC, Mohammad Haniff, MAS, Mohd Razip Wee, MF, Dee, CF, Goh, BT, Mohamed, MA, Majlis, BYM 2017, Reduced graphene oxide preparation and its applications in solution-processed write-once-read-many-times graphene-based memory device, Carbon vol. 124, pp. 547-554.

Seman, RNAR, Azam MA, Mohamed, MA 2016, Highly efficient growth of vertically aligned caron nanotubes on Fe-Ni based metal alloy foils for supercapacitors. *Advances in Natural Sciences:*

Nanoscience and Nanotechnology, vol. 7, no. 4, pp. 045016.

Seo, T, Park, A, Park, S, Kim, Y, Lee, G, Kim, M, Jeong, M, Lee, Y, Hahn, Y & Suh, E 2015 Direct growth of GaN layer on carbon nanotube-graphene hybrid structure and its application for light emitting diodes, *Scientific Reports*, vol. 5, no. 1.

Shao, J, Lv, W, Guo, Q, Zhang, C, Xu, Q, Yang, Q & Kang, F 2012, Hybridization of graphene oxide and carbon nanotubes at the liquid/air interface, *Chem. Commun.*, vol. 48, no. 31, pp. 3706-3708.

Yang, Z, Tian, ., Yin, Z, Cui, C, Qian, W & Wei, F 2019, Carbon nanotube- and graphene-based nanomaterials and applications in high-voltage supercapacitor: A review, *Carbon*, vol. 141, pp.467-480.

Yu, D & Dai, L 2009, Self-assembled graphene/carbon nanotube hybrid films for supercapacitors, *The Journal of Physical Chemistry Letters*, vol. 1, no. 2, pp. 467-470.

Zhu, X, Ning, G, Fan, Z, Gao, J, Xu, C, Qian, W & Wei, F 2012, One-step synthesis of a graphene-carbon nanotube hybrid decorated by magnetic nanoparticles, *Carbon*, vol. 50, no. 8, pp. 2764-2771.